Grand unification scale *CP* violating phases and the electric dipole moment

E. Accomando, R. Arnowitt, and B. Dutta

Center For Theoretical Physics, Department of Physics, Texas A&M University, College Station Texas 77843-4242
(Received 28 July 1999; published 8 May 2000)

The question of *CP* violating phases in supersymmetry and electric dipole moments (EDMs) is considered within the framework of supergravity grand unification (GUT) models with a light ($\lesssim 1$ TeV) mass spectrum. In the minimal model, the nearness of the *t*-quark Landau pole automatically suppresses the *t*-quark cubic soft breaking phase at the electroweak scale. However, current EDM data require the quadratic soft breaking phase to be small at the electroweak scale unless $\tan\beta$ is small ($\tan\beta \lesssim 3$), and the EDM data combined with the requirement of electroweak symmetry breaking require this phase to be both large and highly fine-tuned at the GUT scale unless $\tan\beta$ is small. Nonminimal models are also examined and generally show the same behavior.

I. INTRODUCTION

The standard model (SM) of strong and electroweak interactions possesses only one source of *CP* violating phases: the phase in the Cabibbo-Kobayashi-Maskawa (CKM) matrix. While the physical origin of this phase remains unknown, it appears to satisfactorily account for the observed *CP* violation in the *K* meson system, and future data from *B* factories and high energy accelerators will be able to test its validity for *B*-meson phenomena. It was early on realized that supersymmetric (SUSY) extensions of the standard model allowed for an array of new *CP* violating phases and that these phases could give large contributions to the electric dipole moments (EDMs) of the electron and neutron [1], thus violating the known experimental bounds [2,3]. Several resolutions to this problem have been proposed: e.g., one might assume that the phases are quite small, i.e., $\lesssim O(10^{-2})$ [1,4] or suppress the diagrams by assuming that the relevant SUSY particles are very heavy [5]. Both these suggestions *a priori* appear unsatisfactory: i.e., the first possibility would appear to require a significant amount of fine-tuning, and the second would imply a SUSY spectrum in the TeV domain, possibly beyond the reach of even the CERN Large Hadron Collider (LHC). More recently, it has been realized that some cancellations can occur in different contributions to the EDMs in certain parts of the SUSY parameter space [6], which has led to considerable examination of this possibility [6–15]. In the minimal supersymmetric extension of the SM, the minimal supersymmetric standard model (MSSM) (which we define as the low energy SUSY extension of the SM obtained by supersymmetrizing the particle spectrum with two Higgs doublets), this does appear to reduce the amount of fine-tuning needed, allowing for larger phases. The existence of such phases could also have effects on other predictions of the MSSM [16–21], thus allowing future experimental checks of this idea.

In this paper we consider these questions from the viewpoint of supergravity (SUGRA) grand unified theories (GUTs). In particular we consider gravity mediated models with *R*-parity invariance, where supersymmetry is broken in a hidden sector at some scale above the GUT scale M_G (presumably at the string or Planck scale M_{Pl},) the breaking being transmitted to the physical sector by gravity [22]. (For previous work from this viewpoint see Refs. [6,7,9, 10,13,14].) Such models are much more constrained than the MSSM. Thus low energy properties are now determined by running the renormalization group equations (RGEs) from M_G to the electroweak scale. *CP* violating phases that in the MSSM are arbitrary parameters now get correlated by the RGEs and no longer can be assigned independently to satisfy the EDM experimental bounds. Further, the radiative breaking of SU(2)×U(1) puts additional constraints on the *CP* violating phases. We find that as a consequence of these constraints, one must still fine-tune some of the *CP* violating phases at the electroweak scale to be quite small, except for small regions of the parameter space with $\tan\beta$ close to its minimum value or when SUSY masses are very large. Further, except for the lowest $\tan\beta$ a serious fine-tuning develops at the GUT scale. These phenomena appear to be true both for the minimal SUGRA (MSUGRA) model with universal soft breaking masses and with nonuniversal soft breaking extensions. Hence the required smallness of the phases also tends to reduce the possibility of collateral evidence in other phenomena for their existence in SUGRA models.

In Sec. II, we discuss the solutions of the RGEs for MSUGRA models and explain which phases that are large at the GUT scale get naturally suppressed at the electroweak scale (and which do not) and what the constraints of electroweak breaking imply both at the tree and one-loop level. We then examine the amount of fine-tuning needed to satisfy the existing EDM data and what would be needed if those data were improved by a factor of 10 without finding any EDM. Section III considers some effects of nonuniversal soft breaking on the EDM results.

In gravity-mediated SUGRA models, the structure of the soft breaking parameters is to be deduced from the nature of the Kahler potential and gauge kinetic function at the GUT scale [22–24]. Thus what might be reasonable sizes for *CP* violating phases are presumably Planck scale physics questions. While at present there is no theory of such phenomena, one can still examine the general framework to see under what circumstances small or large phases might occur ''naturally'' at the GUT scale. This is analyzed in Sec. IV, and a
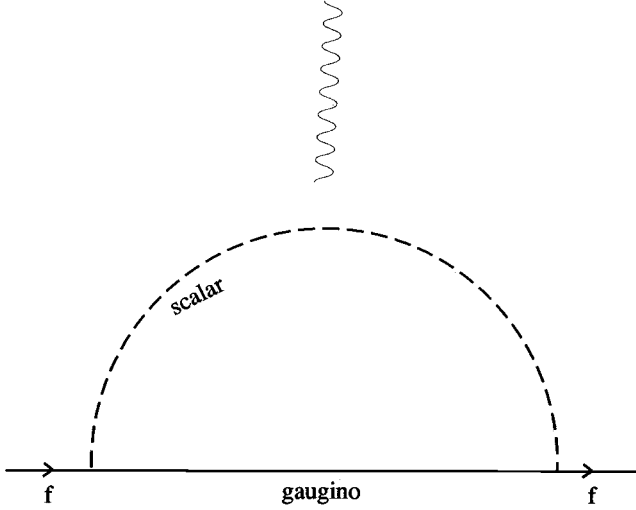
61 115003-1

FIG. 1. One-loop diagram. The photon line can be attached to any charged particle.

model with ''naturally'' small CP violating phases is discussed.

Concluding remarks are given in Sec. V.

II. EDM FOR MSUGRA MODELS

A. EDM diagrams and phases in MSUGRA models

Supergravity GUT models with universal soft breaking of supersymmetry, MSUGRA, depend upon five parameters at the GUT scale: $m_{1/2}$ (the universal gaugino mass), A_0 (the cubic soft breaking mass), B_0 (the quadratic soft breaking mass), μ_0 (the Higgs mixing parameter), and m_0 (the universal squark and slepton mass). Of these, the first four may be complex. However, it is always possible to make a phase transformation on the gaugino fields to make $m_{1/2}$ real, and since the reality is preserved by the RGEs at one-loop order, we will assume for now on that $m_{1/2}$ is real. We parametrize the remaining phases at M_G by

$$A_0 = |A_0| e^{i\alpha_{0A}}, \quad B_0 = |B_0| e^{i\theta_{0B}}, \quad \mu_0 = |\mu_0| e^{i\theta_{0\mu}}. \quad (1)$$

The RGEs allow one to determine the low energy parameters in terms of those of Eq. (1) and $m_{1/2}$ and m_0. Thus at the electroweak scale, one obtains a different A parameter for each fermion (A_u, A_d, A_t, A_b, A_e, and A_τ), real gaugino masses $\tilde{m}_3$, $\tilde{m}_2$, and $\tilde{m}_1$ for the SU(3)$_C$, SU(2)$_L$, and U(1)$_Y$ sectors, and complex B and μ parameters.

The EDM, d_f for fermion f, appears in the effective Lagrangian L_f as

$$L_f = -\frac{i}{2} d_f \bar{f} \sigma_{\mu\nu} \gamma^5 f F^{\mu\nu}. \quad (2)$$

The basic diagrams giving rise to d_f are shown in Fig. 1 and involve neutralino ($\tilde{\chi}_i^0$, $i=1,4$), chargino ($\tilde{\chi}_i^\pm$, $i=1,2$), and gluino ($\tilde{g}$) loops with squarks ($\tilde{q}$) and sleptons ($\tilde{l}$).

For the neutron dipole moment d_n one must also take into account the gluonic operators
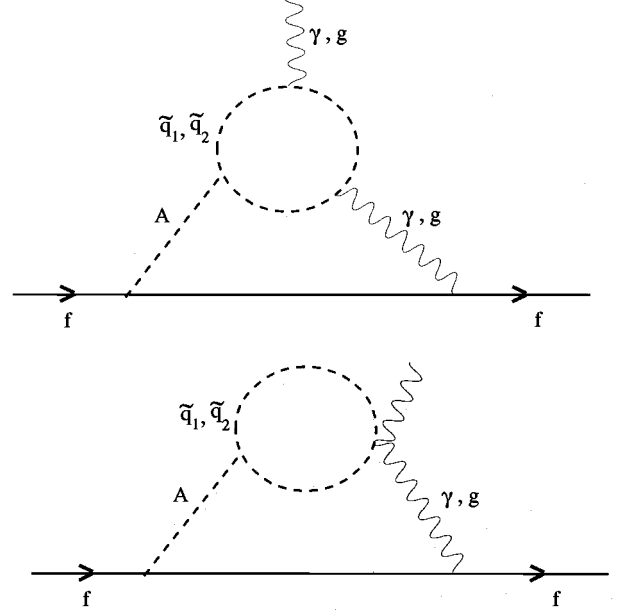

FIG. 2. Two-loop Barr-Zee diagrams. A is the CP-odd Higgs boson and $\tilde{q}_i$ are the mass diagonal squark states.

$$L^G = -\frac{1}{3} d^G f_{abc} G_{a\mu\alpha} G_{b\nu}^\alpha \tilde{G}_c^{\mu\nu} \quad (3)$$

and

$$L^C = -\frac{i}{2} d^C \bar{q} \sigma_{\mu\nu} \gamma^5 T^a q G_a^{\mu\nu}, \quad (4)$$

where $\tilde{G}_c^{\mu\nu} = \frac{1}{2} \epsilon^{\mu\nu\alpha\beta} G_{c\alpha\beta}$, f_{abc} are the SU(3) structure constants, and $T^a = \frac{1}{2} \lambda^a$, where λ^a are the SU(3) Gell-Mann matrices. In addition to the diagrams of Fig. 1 with γ replaced by g, operators of Eqs. (2)–(4) receive contributions from the two-loop Barr-Zee diagrams of Fig. 2 [25], and the two-loop Weinberg-type diagram of Fig. 3 [26]. For the neutron dipole moment one must use the QCD factors $\eta^{ED}, \eta^G, \eta^C$ to evolve the results at the electroweak scale down to 1 GeV [27].

The calculation of d_n suffers from QCD uncertainties from several sources. These include the following.
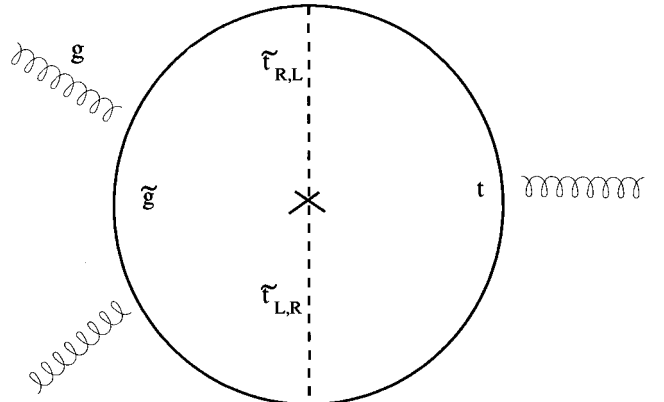

FIG. 3. Two-loop Weinberg-type diagram.

(1) How to relate the quark moments d_u, d_d to the neutron moment d_n. We use here the nonrelativistic quark model relation (for other approaches see Refs. [14,28,29]):

$$d_n = \frac{1}{3}(4d_d - d_u). \tag{5}$$

(2) How to relate color and gluonic contributions to the electric dipole moment. We use here the ''naive dimensional analysis'' of Ref. [30].

(3) Uncertainty in m_s, the strange quark mass, which affects the determination of m_u and m_d. While the quark mass ratios are well known [31],

$$\frac{m_u}{m_d} = 0.553 \pm 0.043, \quad \frac{m_s}{m_d} = 18.9 \pm 0.8, \tag{6}$$

one has $m_s = (175 \pm 25)$ MeV from QCD sum rules and $m_s = (100 \pm 20 \pm 10)$ MeV (2 GeV) from the quenched lattice calculation [32]. (Using unquenched approximation one expects an even smaller value [33].)

Thus the values of d_n calculated below have a significant uncertainty. In spite of this, it is useful to see the effect on the SUSY parameter space of simultaneously imposing the

experimental constraints on both d_n and d_e and we will discuss below how the uncertainty in m_s effects these constraints.

To specify our phase conventions, we give the mass matrices for the particles entering in Fig. 1. With a convenient choice of phases, the chargino and the neutralino mass matrices are

$$M_{\chi^{\pm}} = \begin{pmatrix} \tilde{m}_2 & \sqrt{2}M_W \sin\beta \\ \sqrt{2}M_W \cos\beta & -|\mu|e^{i\theta} \end{pmatrix}, \tag{7}$$

$$M_{\chi^0} = \begin{pmatrix} \tilde{m}_1 & 0 & a & b \\ 0 & \tilde{m}_2 & c & d \\ a & c & 0 & |\mu|e^{i\theta} \\ b & d & |\mu|e^{i\theta} & 0 \end{pmatrix}, \tag{8}$$

where $a = -M_Z \sin\theta_W \cos\beta$, $b = M_Z \sin\theta_W \sin\beta$, $c = -\cot\theta_W a$, $d = -\cot\theta_W b$, $\tan\beta = v_2/v_1$ ($v_{1,2} = |\langle H_{1,2} \rangle|$), and θ_W is the weak mixing angle. The phase θ is given by

$$\theta = \epsilon_1 + \epsilon_2 + \theta_\mu, \tag{9}$$

where at the electroweak scale, $\langle H_{1,2} \rangle = v_{1,2} e^{i\epsilon_{1,2}}$, and $\mu = |\mu|e^{i\theta_\mu}$. The squark mass matrices may be written as

$$M_{\tilde{q}}^2 = \begin{pmatrix} m_{\tilde{q}_L}^2 & e^{-i\alpha_q}m_q(|A_q| + |\mu|R_q e^{i(\theta+\alpha_q)}) \\ e^{i\alpha_q}m_q(|A_q| + |\mu|R_q e^{-i(\theta+\alpha_q)}) & m_{\tilde{q}_R}^2 \end{pmatrix}, \tag{10}$$

where m_q and e_q are the quark mass and charge,

$$m_{\tilde{q}_L}^2 = m_Q^2 + m_q^2 + (1/2 - e_q \sin^2\theta_W)M_Z^2 \cos 2\beta, \tag{11}$$

$$m_{\tilde{q}_R}^2 = m_U^2 + m_q^2 + e_q \sin^2\theta_W M_Z^2 \cos 2\beta, \tag{12}$$

$A_q = |A_q|e^{i\alpha_q}$, m_Q^2 and m_U^2 are given in Ibanez *et al.* [34], and $R_q = \cot\beta(\tan\beta)$ for $u(d)$ quarks. Similar expressions hold for slepton masses, with phases α_l. Our sign conventions for A_q and μ are those of Ref. [38].

B. Effective potential and the relation among phases

The condition for electroweak symmetry breaking is obtained by minimizing the effective potential V_{eff} with respect to v_1, ϵ_1, v_2, and ϵ_2. The Higgs sector of V_{eff} is

$$V_{\text{eff}} = m_1^2 v_1^2 + m_2^2 v_2^2 + 2|B\mu|\cos(\theta + \theta_B)v_1 v_2$$
$$+ \frac{g^2}{8}(v_1^2 - v_2^2)^2 + \frac{g'^2}{8}(v_2^2 - v_1^2)^2 + V_1, \tag{13}$$

where V_1 is the one-loop contribution, and $m_i^2 = \mu^2 + m_{H_i}^2$ and $m_{H_{1,2}}^2$ are the $H_{1,2}$ running masses. For particles of spin j, one has

$$V_1 = \frac{1}{64\pi^2} \sum_a C_a(-1)^{2j_a}(2j_a + 1)m_a^4 \left(\ln\frac{m_a^2}{Q^2} - \frac{3}{2} \right), \tag{14}$$

where C_a is the color degree of freedom of the ath particle. In the following we choose the low energy scale Q to be m_t (175 GeV) and include the full third generation states t, b, and τ in V_1. This allows an examination of the large $\tan\beta$ domain.

We view the minimization equations of V_{eff} as equations to determine the Higgs vacuum expectation values (VEVs) i.e., $v_1, v_2, \epsilon_1, \epsilon_2$. Thus, in the tree approximation, the extrema equations $\partial V_{\text{eff}}/\partial\epsilon_i = 0$ yield $2|B\mu|\sin(\theta + \theta_B) = 0$, and hence the minimum of V_{eff} requires

$$\theta = \pi - \theta_B \tag{15}$$

(the choice of $\theta = -\theta_B$ leads to a maximum). The one-loop corrections depend only on the mass eigenvalues and, hence from Eq. (10), only on the phase $\theta + \alpha_q$ and $\theta + \alpha_l$. Thus, at the one-loop level, one gets a correction to Eq. (15) of the form [16,17]

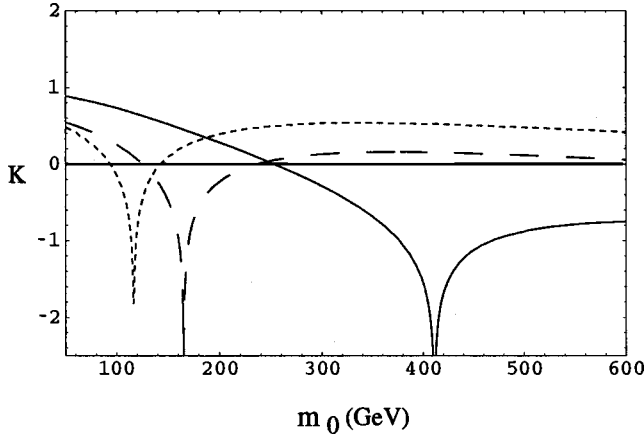$$\theta = \pi - \theta_B + f_1(\pi - \theta_B + \alpha_q, \pi - \theta_B + \alpha_l), \tag{16}$$

FIG. 4. K (defined in the text) is plotted as a function of m_0 for d_e. The solid, dashed, and dotted lines are for $\tan\beta=3$, 10, and 20, respectively. The other input parameters are $\alpha_{0A}=\pi/2$, $|A_0| = 300$ GeV, $\theta_B=0.02$, and $m_{1/2}=300$ GeV.

where f_1 is the one-loop correction with θ approximated by its tree value, Eq. (15). As we will see, this correction can become significant for large $\tan\beta$. The EDMs, however, depend on both the mass eigenvalues and the rotation matrices. Hence they will depend on $\theta+\alpha_q$ and α_q separately, with θ determined by the electroweak symmetry breaking condition in Eq. (16).

C. Results and analysis of fine-tuning of θ_{0B}

The current experimental 90% C.L. upper bounds on d_n [3] and d_e [2] are

$$(d_n)_{\text{expt}} < 6.3 \times 10^{-26} e \text{ cm}, \quad (d_e)_{\text{expt}} < 4.3 \times 10^{-27} e \text{ cm}.$$
(17)

In discussing the data, it is convenient to define the quantity

$$K = \log_{10}\left|\frac{d_f}{(d_f)_{\text{expt}}}\right|.$$
(18)

Thus $K=0$ corresponds to a theoretical value which saturates the current experimental bound, while $K=-1$ would represent the case should the experimental bounds be reduced by a factor of 10. As pointed out in Refs. [6–15], various cancellations can occur among the different contributions to the EDM. This is illustrated in Fig. 4 where K is plotted versus m_0 for the electron electric dipole moment (EEDM). We note that eventually for very large m_0, the curves fall below the $K=0$ bound (as expected). Further, the allowed range of m_0 (so that $K\lesssim 0$) decreases with increasing $\tan\beta$ (and the allowed range would become very small should $K=-1$; i.e., the experimental bounds would be reduced by a factor of 10). In addition, the position of the dips moves to lower m_0 with increasing $\tan\beta$. This happens due to the fact that the regions on the right of the dips are dominated by the contribution from the chargino diagram. As $\tan\beta$ increases, the contribution from the chargino diagram increases much more than the contribution from the neutralino diagram. However, a decrease in m_0 increases the

neutralino diagram much more than the chargino diagram. As a result, the dips shift towards the smaller m_0 value for larger $\tan\beta$. We use negative values [arising from the factor π in the Eq. (15)] of μ to satisfy the experimental constraints on the branching ratio (BR) of $b\rightarrow s\gamma$ [35,36]. The restriction in the SUSY parameter space from electroweak data has been considered in Ref. [37]. If the SLAC Large Detector (SLD) measured value of $\sin^2\theta_w$, is used, there is no new bound in the $m_{1/2}$-m_0 plane. The CERN e^+e^- collider LEP average of $\sin^2\theta_w$, however, differs from the SLD measurement by 2.9σ and the combined SLD and LEP can rule out $m_{1/2}$ up to 300 GeV (independent of m_0). Since the difference between the two measurements is significant, we do not restrict the parameter space using this data in this work.

We begin our analysis by examining the RGEs to determine what GUT scale parameters lead to acceptable CP violating phases at the electroweak scale. We have used Ref. [38] for the RGEs relating the GUT scale parameters to the parameters at the electroweak scale. In general, the RGEs must be solved numerically and all results given below are obtained by accurate numerical integration. However, approximate analytic solutions can be found for low and intermediate $\tan\beta$ (neglecting b and τ Yukawa couplings) or for the SO(10) limit of very large $\tan\beta$ (neglecting the τ Yukawa coupling). These analytic solutions give some insight into the nature of the more general numerical results.

The solution for the $A_t(t)$ parameter in the low and intermediate $\tan\beta$ cases can be cast in the form [39]

$$A_0 = \frac{A_R(t)}{D_0} + \frac{H_3(t)}{F(t)}m_{1/2},$$
(19)

where A_R is the residue at the t-quark Landau pole:

$$A_R = A_t + m_{1/2}\left(H_2(t) - \frac{H_3(t)}{F(t)}\right)$$
(20)

and

$$D_0 = 1 - 6\frac{F(t)}{E(t)}Y(t).$$
(21)

Here $t = 2\ln(M_G/Q)$, the form factors E, F, H_2, and H_3 are real and are defined in [34], and $Y(t) = h_t/16\pi^2$, where h_t is the t-quark Yukawa coupling constant. D_0 vanishes at the t-quark Landau pole [for $Q=m_t$, $D_0 \cong 1-(m_t/200\sin\beta)^2$] and is generally small (i.e., $D_0 \lesssim 0.2$ for $m_t = 175$ GeV). The imaginary part of Eq. (19) gives

$$D_0|A_0|\sin\alpha_{0A} = |A_t|\sin\alpha_t.$$
(22)

Thus, even if $\alpha_{0A}=\pi/2$, α_t at the electroweak scale will be generally suppressed due to the smallness of D_0; i.e., the RGEs naturally make the phase α_t small due to the nearness of the Landau pole. (This result has been previously observed, for low $\tan\beta$ in [9].) The approximate SO (10) solution with large $\tan\beta$ (where $Y_t \cong Y_b$) gives a similar analytic form for $A_t(t) \cong A_b(t)$ with the factor 6 replaced by 7 in Eq. (21). Thus the suppression effect on α_t occurs over the
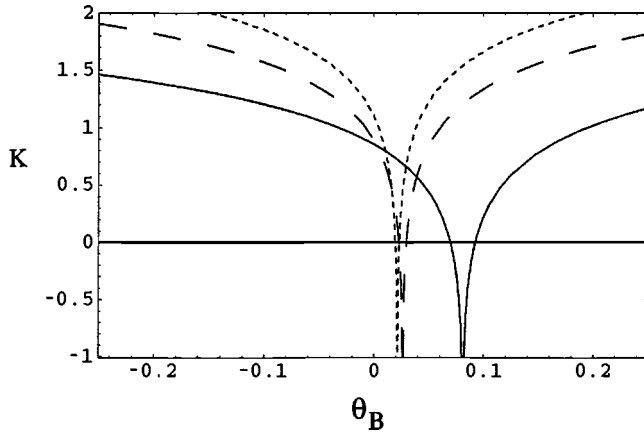
FIG. 5. K (for EEDM) is plotted as a function of θ_B. The solid, dashed, and dotted lines are for $\tan\beta=3$, 10, and 20, respectively. The other input parameters are $\alpha_{0A}=\pi/2$, $|A_0|=300$ GeV, $m_{1/2}=300$ GeV, and $m_0=100$ GeV.

entire $\tan\beta$ domain. These effects thus allow α_{0A} to be large without a priori violating the experimental EDM bounds.

In contrast, there is no analogous RGE suppression effect in the first generation A parameters A_u, A_d, and A_e. From the RGEs, one finds that A_u has the form of Eq. (19) for low and intermediate $\tan\beta$ with the factor 6 replaced by 1 in Eq. (21). Now $D_0\simeq1$ and no suppression effect occurs for α_u at the electroweak scale in the analogue of Eq. (22). However, the EDMs are not very sensitive to the first generation α_u, α_d, α_e and one can have large values of these parameters without violating the experimental bounds in a reasonable region of the SUSY parameter space.

From the RGE, one sees that the phase of the μ parameter does not run at the one-loop level, i.e., $\theta_{0\mu}=\theta_\mu$, where θ_μ is the phase at the electroweak scale. Thus a large GUT scale phase will lead to a large electroweak scale phase. However, as seen in Eqs. (7)–(10), θ_μ enters only in the combination θ, and θ is determined in terms of θ_B, α_l, and α_q by the minimization of the effective potential, as given in Eq. (16). Thus (with our choice of the phases in the mass matrices) θ_μ does not enter in the EDMs.

The EDMs, however are highly sensitive to θ_B, which, by Eq. (16), enters into all the diagrams, and over most of the parameter space, θ_B must be small to satisfy the EDM experimental bounds. This is illustrated in Fig. 5 where we have plotted the EEDM K vs θ_B. We see that θ_B can be large, i.e., $\theta_B\simeq0.08$, for low $\tan\beta=3$, though it becomes smaller for higher $\tan\beta$. However, even for $\tan\beta=3$, the range $\Delta\theta_B$ of θ_B so that $K\lesssim0$ is very small, i.e., $\Delta\theta_B\lesssim0.02$ (and θ_B would become quite fine tuned if the experimental bound were reduced by a factor of 3, i.e., $K=-0.5$). Figure 6 shows that $\Delta\theta_B$ remains small for $m_{1/2}\lesssim350$ GeV ($m_{\tilde{g}}\lesssim1$ TeV) and only relaxes somewhat when $m_{1/2}\simeq700$ GeV ($m_{\tilde{g}}\lesssim2$ TeV). In this figure we have plotted the $K\lesssim0$ regions as a function of θ_B and $m_{1/2}$ for three different values of $\tan\beta$. Since the contribution from the chargino diagram increases with $\tan\beta$, the larger $\tan\beta$ requires a smaller phase to produce the necessary cancellation between the chargino and the neutralino diagrams.
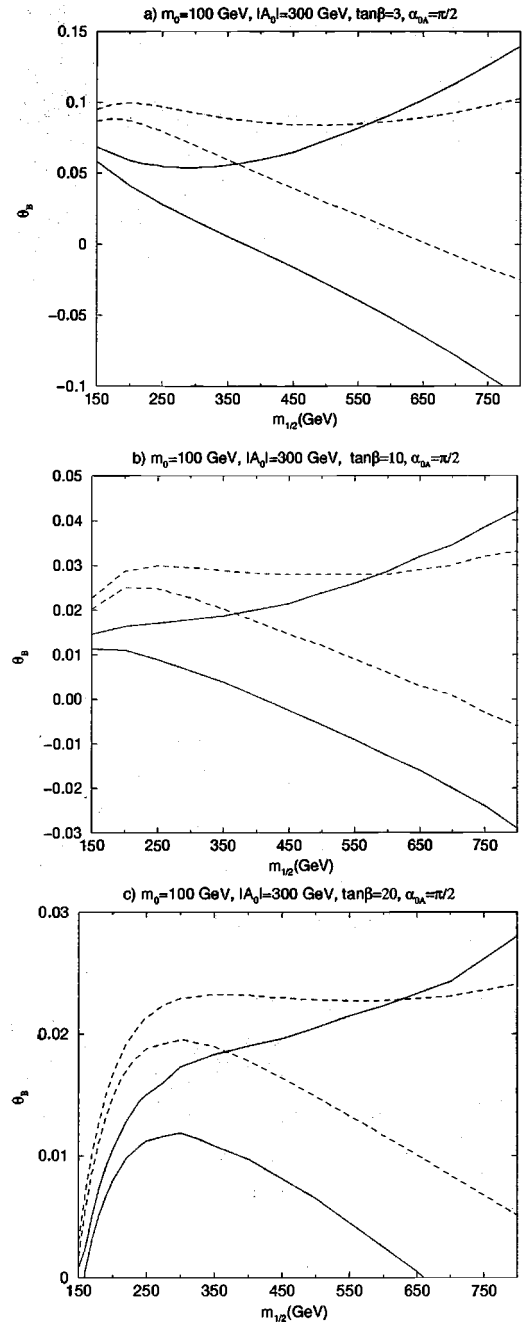

FIG. 6. The $K=0$ contours plotted as a function of θ_B and $m_{1/2}$. The solid lines are for d_n, and the dotted lines are for d_e.

The RGEs allow us to examine the significance of the above results at the GUT scale. The RGEs for B and A_t can be solved in the low and intermediate $\tan\beta$ regime to obtain

$$B=B_0-\frac{1}{2}(1-D_0)A_0-\Phi m_{1/2}, \qquad (23)$$

where

$$\Phi=-\frac{1}{2}(1-D_0)\frac{H_3}{F}+\left[3h_2+\frac{3}{5}h_1\right]\frac{\alpha_G}{4\pi}, \qquad (24)$$

$h_i = t/(1+\beta_i t)$, $\alpha_G \cong 1/24$ is the GUT gauge coupling constant, and β_i are the MSSM beta functions. The real and imaginary parts of Eq. (23) give

$$|B|\sin\theta_B = |B_0|\sin\theta_{0B} - \frac{1}{2}(1-D_0)|A_0|\sin\alpha_{0A}, \quad (25)$$

$$|B|\cos\theta_B = |B_0|\cos\theta_{0B} - \frac{1}{2}(1-D_0)|A_0|\cos\alpha_{0A} - \Phi m_{1/2}. \quad (26)$$

Equations (25),(26) can be viewed as determining the electroweak scale values of $|B|$ and θ_B in terms of the GUT input parameters. Thus θ_B depends upon both the initial phase θ_{0B} and the A_0 phase α_{0A}. Alternatively, one may use Eqs. (25),(26) to impose electroweak scale phenomenological constraints on the allowed GUT parameters. The requirement that the GUT theory give rise to electroweak symmetry breaking gives

$$|B| = \frac{1}{2}\sin 2\beta \frac{m_3^2}{|\mu|}, \quad (27)$$

where $m_3^2 = \mu_1^2 + \mu_2^2$ and $\mu_i^2 = |\mu|^2 + m_{H_i}^2 + \Sigma_i$. (Here $m_{H_i}^2$ are the running Higgs boson masses at the electroweak scale, $|\mu|$ is determined by electroweak breaking, and Σ_i are the one-loop corrections [40].) In addition, we have seen that the experimental bounds on the EDMs restrict θ_B to be small, i.e., $|\theta_B| \lesssim 0.1$ (and usually much smaller), and the allowed range $\Delta\theta_B$, which satisfies the EDMs, is quite small. These conditions put severe constraints on the GUT scale theory which we now discuss.

Consider first the case where $\tan\beta$ is very close to its minimum value, e.g., $\tan\beta = 2$. Here $\sin 2\beta/2$ is not small, and by Eq. (27), $|B|$ is of normal size. Equation (25) then implies that θ_B and θ_{0B} are of roughly the same size (even for $\alpha_{0A} = \pi/2$) as previously noted in Ref. [9]. Thus a reasonable GUT theory requires one only to justify the size of θ_{0B}. However, as $\tan\beta$ increases, $1/2\sin 2\beta$ decreases, and unless μ becomes anomalously small or m_3^2 anomalously large, Eq. (27) implies that $|B|$ becomes small. Thus the left-hand side of Eq. (25) becomes small (and to first approximation can be neglected), and Eq. (25) implies that θ_{0B} is determined by α_{0A} mainly; i.e., θ_{0B} is large if α_{0A} is large. This result is illustrated in Fig. 7 where θ_{0B} is plotted vs θ_B. We see that since θ_B is small for all $\tan\beta$, θ_{0B} is in general large: e.g., even for $\tan\beta = 3$, one has $\theta_{0B} \simeq 0.8$.

Returning to Eq. (25), we see, however, that $\Delta\theta_{0B}$, the range of values of θ_{0B} that will satisfy the EDM constraints, is very small. Thus, for fixed A_0, Eq. (25) implies for large $\tan\beta$ that

$$\Delta\theta_{0B} \cong \frac{|B|}{|B_0|}\Delta\theta_B \ll \Delta\theta_B, \quad (28)$$

and since $\Delta\theta_B$ is small, $\Delta\theta_{0B}$ will be very small. This is illustrated in Fig. 8 where the allowed values of θ_{0B} for $K \lesssim 0$ are plotted vs $m_{1/2}$ for d_e and d_n for $\tan\beta = 3,10,20$. We
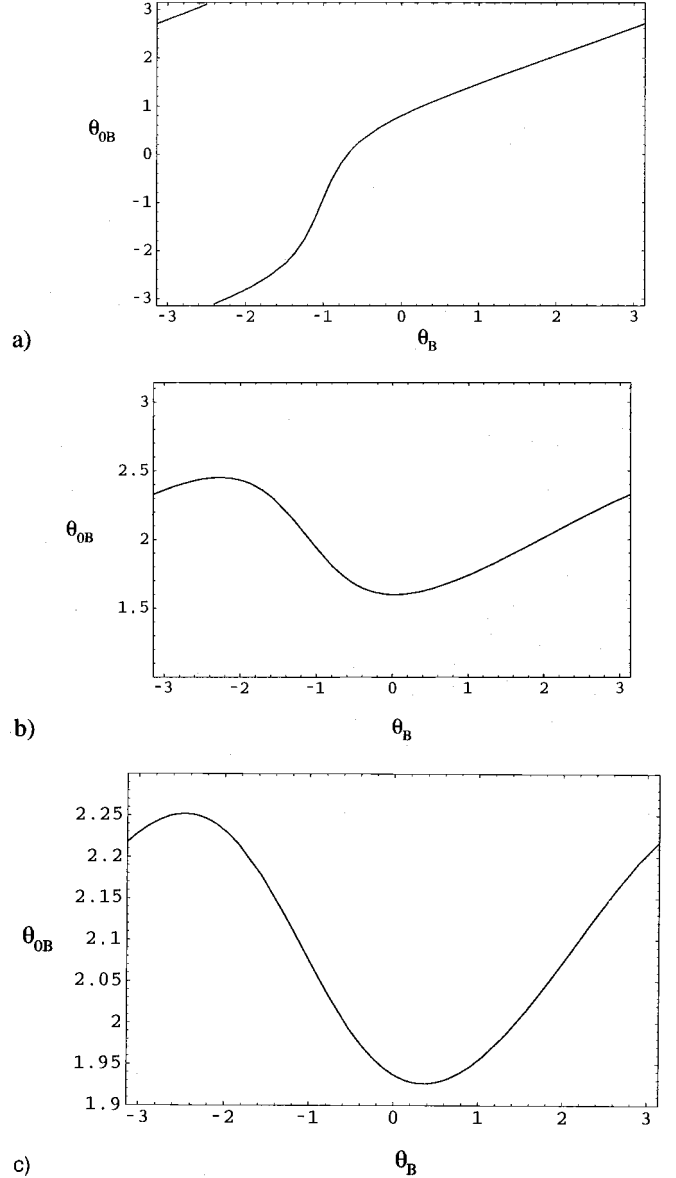
a)

b)

c)

FIG. 7. θ_{0B} is plotted as a function of θ_B. (a), (b), and (c) are for $\tan\beta = 3$, 10, and 20, respectively. The other input parameters are $\alpha_{0A} = \pi/2$, $|A_0| = 300$ GeV, $m_0 = 100$ GeV, and $m_{1/2} = 300$ GeV.

see that the phenomenological constraints at the electroweak scale imply that θ_{0B} is both large and its value is sharply fine-tuned (unless α_{0A} is small, SUSY masses are large or $\tan\beta$ is small). One may alternatively view this from the "top down": if Planck physics determines α_{0A} and θ_{0B} to be large and fixed, then if the model is to achieve electroweak symmetry breaking with EDMs below existing bounds, there will be a fine-tuning of other GUT scale parameters (unless $\tan\beta$ is small or the SUSY masses are large).

D. Constraints from simultaneous satisfaction of d_e and d_n bounds

As discussed above, there are a number of uncertainties in the calculation of the neutron EDM. Figure 9 illustrates the
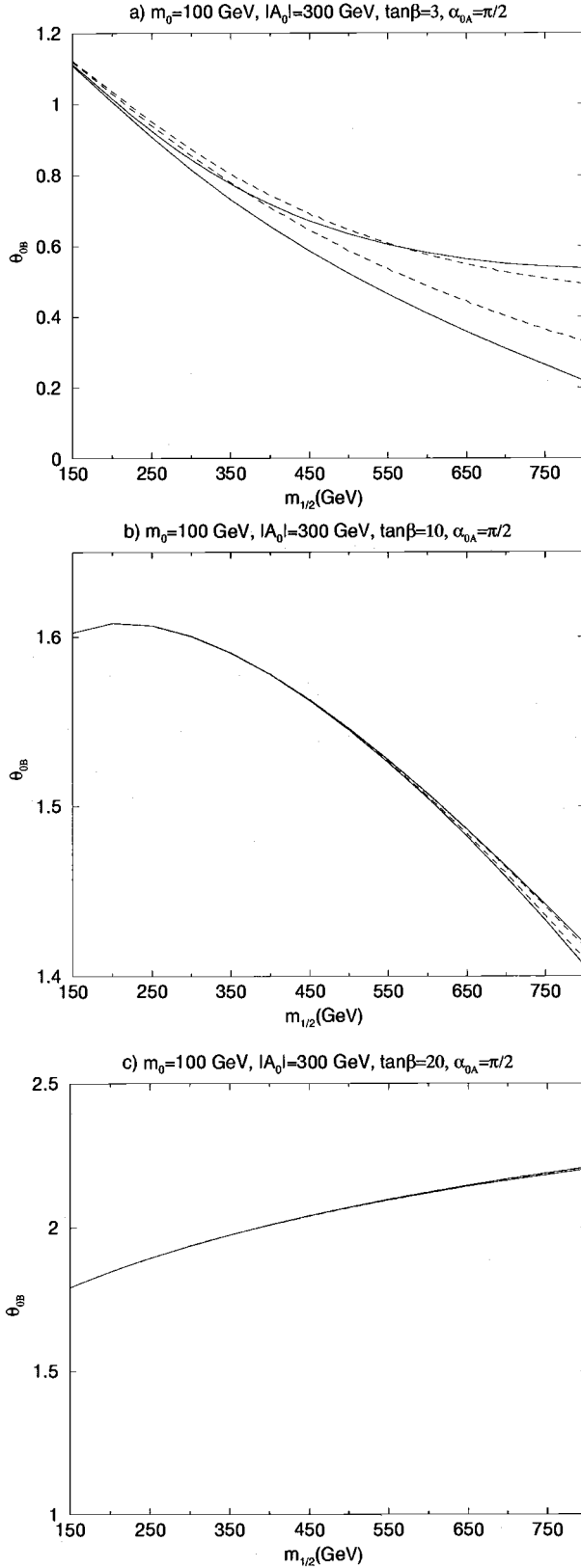
a) $m_0=100$ GeV, $|A_0|=300$ GeV, $\tan\beta=3$, $\alpha_{0A}=\pi/2$

b) $m_0=100$ GeV, $|A_0|=300$ GeV, $\tan\beta=10$, $\alpha_{0A}=\pi/2$

c) $m_0=100$ GeV, $|A_0|=300$ GeV, $\tan\beta=20$, $\alpha_{0A}=\pi/2$
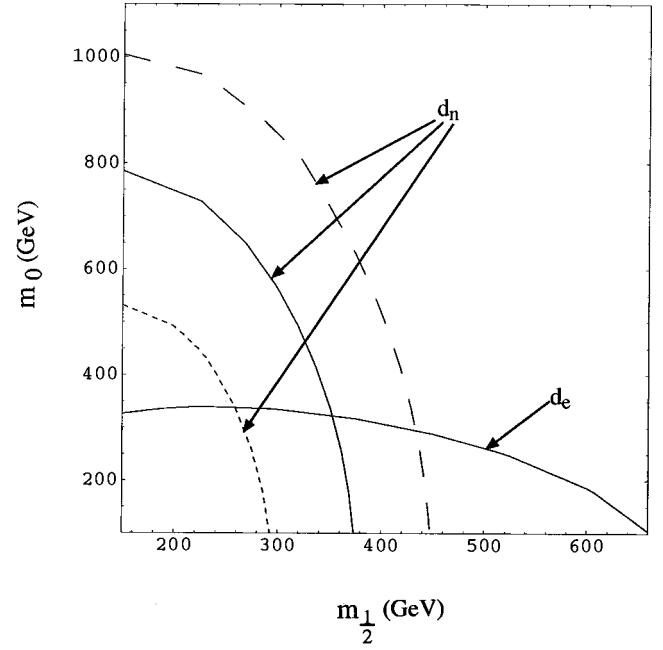

FIG. 9. The $K=0$ contours are plotted as a function of m_0 and $m_{1/2}$. The dotted, solid, and dashed lines are for m_d (1 GeV)=5, 8, and 12 MeV, respectively. The other input parameters are $\alpha_{0A}=\pi/2$, $|A_0|=300$ GeV, $\theta_B=0$, and $\tan\beta=3$. Excluded regions are below d_e and to the left of the d_n curves.

effects of varying the d-quark mass in a plot of the region allowed by the experimental EDM bounds ($K\leq0$) in the m_0-$m_{1/2}$ plane for $\theta_B=0$, $|A_0|=300$ GeV, $\alpha_{0A}=\pi/2$, $\tan\beta=3$. The bound on d_e already excludes all regions below the lower solid curve, while the d_n bound excludes regions to the left of the upward running curves for $m_d=5$ MeV (dotted line), $m_d=8$ MeV (solid line), $m_d=12$ MeV (dashed line). Thus the combined exclusion region increases from $m_{1/2}\gtrsim260$ GeV to $m_{1/2}\gtrsim440$ GeV as m_d increases, a significant change. In the other figures in this paper we have used the middle value of $m_d=8$ MeV corresponding to $m_s\simeq150$ MeV.

In Fig. 9, we have chosen $\theta_B=0$. As one increases θ_B, one will eventually arrive at a neutralino-chargino cancellation region, and this will reduce the values of m_0 and $m_{1/2}$ which are excluded. Further, for low $\tan\beta$ this cancellation can occur at relatively large θ_B (i.e., $\theta_B\simeq0.2$) as shown in Ref. [9]. Alternatively, increasing $\tan\beta$ can also cause this cancellation, as the loop corrections, Eq. (16), become large with large $\tan\beta$ and the contribution from the chargino diagram increases with $\tan\beta$. This is illustrated for $\tan\beta=20$ in Fig. 10 where the d_n curve for $K=0$ (solid line) bends downward below $m_0=500$ GeV when 200 GeV$<m_{1/2}$ <400 GeV, showing in this exceptional type situation that one can satisfy the EDM constraints with a light particle spectrum and large $\tan\beta$. Note that the cancellation can occur for a relatively wide band of $m_{1/2}$, and persists even for $K=-0.5$.

The regions of the SUSY parameter space that get eliminated by a joint imposition of the experimental bounds on the d_e and d_n are sensitive, of course, to the choice of the
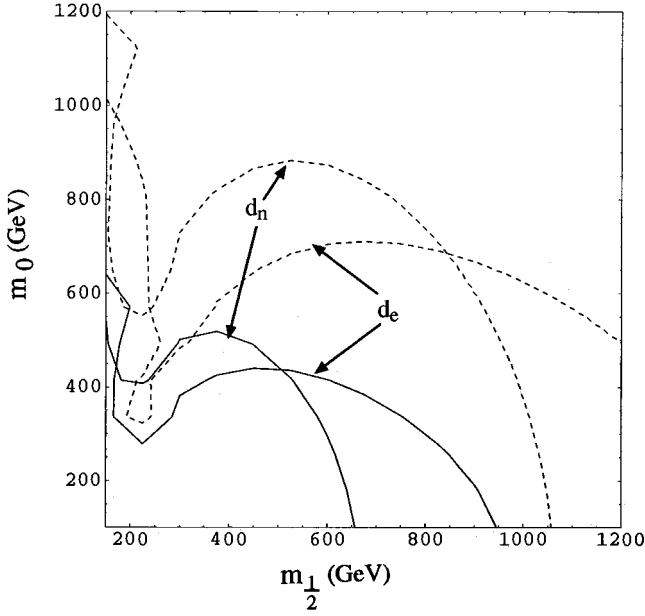
FIG. 8. θ_{0B} vs $m_{1/2}$. Upper and lower lines are the allowed range so that $K\leq0$. The solid lines are for d_n, and the dotted lines are for d_e.

FIG. 10. Allowed region in the m_0-$m_{1/2}$ plane for d_e and d_n. The other input parameters are $\alpha_{0A} = \pi/2$, $|A_0| = 300$ GeV, $\theta_B = 0$, and $\tan\beta = 20$. The solid lines are for $K = 0$, and the dotted lines are for $K = -0.5$.

FIG. 12. The $K = 0$ contours are plotted as a function of θ_B and $m_{1/2}$, where $\alpha_{0A} = \pi/2$, $|A_0| = 800$ GeV, $m_0 = 100$ GeV, and $\tan\beta = 3$. The solid lines are for d_n, and the dotted lines are for d_e.

parameters. Thus in Fig. 6 one sees that for $m_0 = 100$ GeV, one requires $m_{1/2} \gtrsim 350$ GeV ($m_{\tilde{g}} \gtrsim 1$ TeV) to jointly satisfy the d_e and d_n bounds, and this requirement is roughly independent of $\tan\beta$. Figure 11 shows that if m_0 is increased to 250 GeV, one requires now $m_{1/2} \gtrsim 160$ GeV ($m_{\tilde{g}} \gtrsim 450$ GeV) to satisfy both bounds; i.e., if m_0 is increased, the lower bound on $m_{1/2}$ is decreased as expected. However, if $|A_0|$ is increased, it is not necessary that the allowed do-
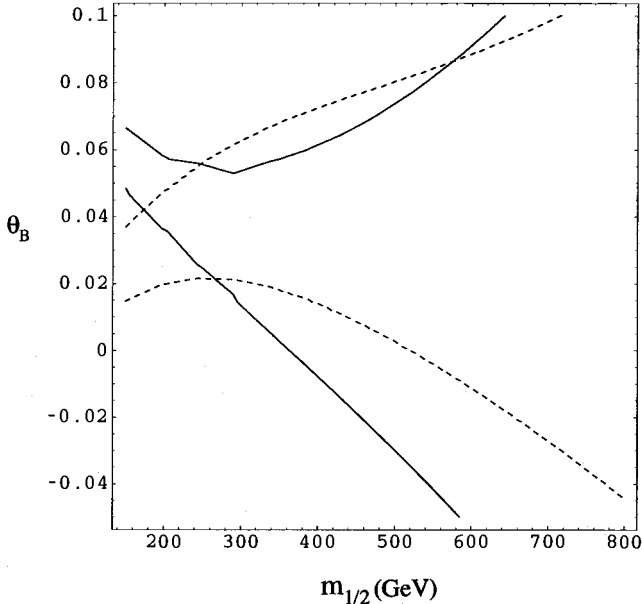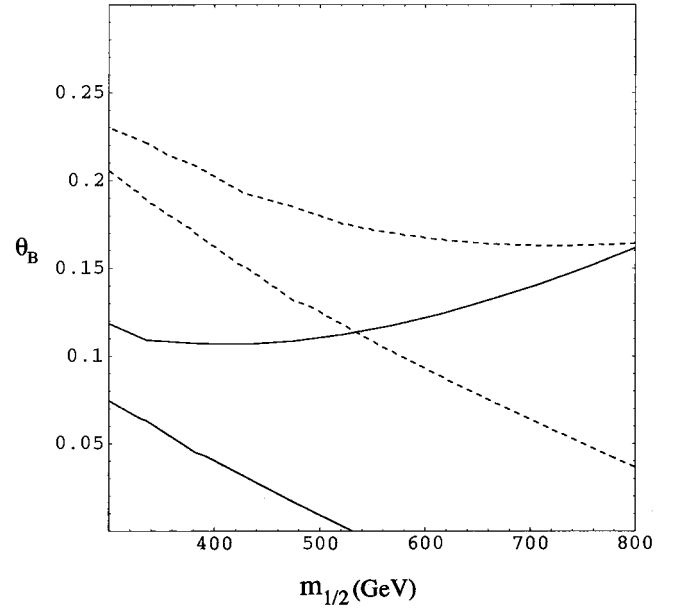
main of $m_{1/2}$ increase. This is illustrated in Fig. 12 for the choice $|A_0| = 800$ GeV, $m_0 = 100$ GeV. The increase of $|A_0|$ raises the allowed values of θ_B for both d_e and d_n, but the raising of d_e is larger causing the joint allowed domain to require $m_{1/2} \gtrsim 550$ GeV ($m_{\tilde{g}} \gtrsim 1.5$ TeV).

In order to exhibit the size of $|\mu|$, we have plotted $|\mu|$ as a function of $m_{1/2}$ for $m_0 = 100$, 300, and 700 GeV in Fig. 13. The EDM constraints have not been imposed in Fig. 13, but from Fig. 6a, one sees that they are satisfied at least for $m_0 = 100$ GeV for d_e for essentially the entire $m_{1/2}$ range (which allows $\theta_B \simeq 0.08$). Note that $|\mu|$ is large (i.e., $|\mu|^2/M_Z^2 \gg 1$) over the full $m_{1/2}$ domain so that one is generally in the gaugino scaling domain.

III. NONUNIVERSAL SOFT BREAKING

There are three types of nonuniversalities that might be considered in SUGRA models: nonuniversal gaugino masses at M_G, nonuniversal scalar masses at M_G, and generation off-diagonal cubic soft breaking matrices A_{ij} and scalar mass matrices m_{ij}^2. We will discuss here briefly the first two possibilities: a more detailed analysis will be given in a later paper [41]. (The third type of nonuniversality has the possibility of generating ϵ and ϵ'/ϵ CP violations independent of the CKM phase [42].)

In general, the U(1), SU(2), and SU(3) gaugino masses at M_G can have the form

$$m_{1/2i} = |m_{1/2i}| e^{i\phi_i}, \quad i = 1,2,3. \tag{29}$$

A convenient phase choice is to set the SU(2) phase to zero $\phi_2 = 0$, and hence the chargino mass matrix, Eq. (7), is unchanged. The remaining phases produce effects in the RGFs for $A_t(t)$:
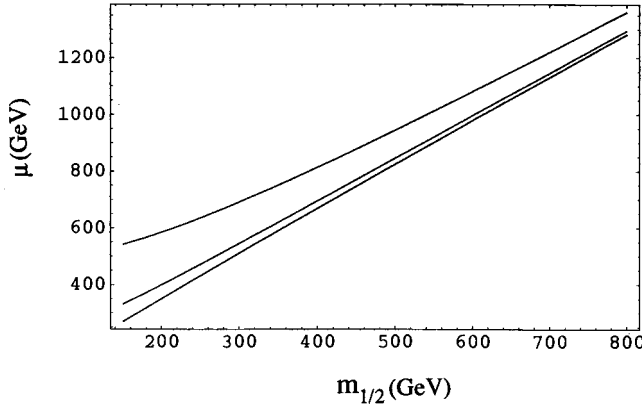

FIG. 11. The $K = 0$ contours are plotted as a function of θ_B and $m_{1/2}$, where $\alpha_{0A} = \pi/2$, $|A_0| = 300$ GeV, $m_0 = 250$ GeV, and $\tan\beta = 3$. The solid lines are for d_n, and the dotted lines are for d_e.

FIG. 13. The parameter $|\mu|$ is plotted as a function of $m_{1/2}$. The three solid lines are for $m_0 = 700$ (top), 300 (middle), and 100 (bottom) GeV. The other input parameters are $\alpha_{0A} = \pi/2$, $|A_0| = 300$ GeV, $\tan\beta = 3$, and $\theta_B = 0.08$.

$$A_t = D_0 A_0 + \sum_i \Phi_{ti} |m_{1/2i}| e^{i\phi_i}, \tag{30}$$

and hence the imaginary part gives

$$|A_t| \sin\alpha_t = |A_0| D_0 \sin\alpha_{0A} + \sum_i \Phi_{ti} |m_{1/2i}| \sin\phi_i. \tag{31}$$

Thus the Landau pole factor D_0 still suppresses any large phase α_{0A} at the GUT scale, though α_t may become large due to the ϕ_i phase which does not run at one-loop order and hence is not suppressed. This phenomena can affect d_n.

A second effect occurs in the neutralino mass matrix which now reads

$$M_{\chi^0} = \begin{pmatrix} |\tilde{m}_1| e^{i\phi_1} & 0 & a & b \\ 0 & \tilde{m}_2 & c & d \\ a & c & 0 & |\mu| e^{i\theta} \\ b & d & |\mu| e^{i\theta} & 0 \end{pmatrix}, \tag{32}$$
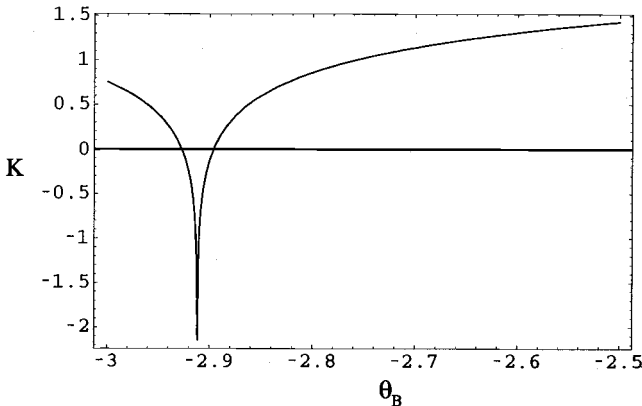

FIG. 14. K (for d_e) as a function of θ_B. The other input parameters are $m_0 = 200$ GeV, $m_{1/2i} = 150$ GeV, $\tan\beta = 3$, $\alpha_{0A} = \pi/2$, $|A_0| = 100$ GeV, and $\phi_1 = 4\pi/5 = \phi_3$.
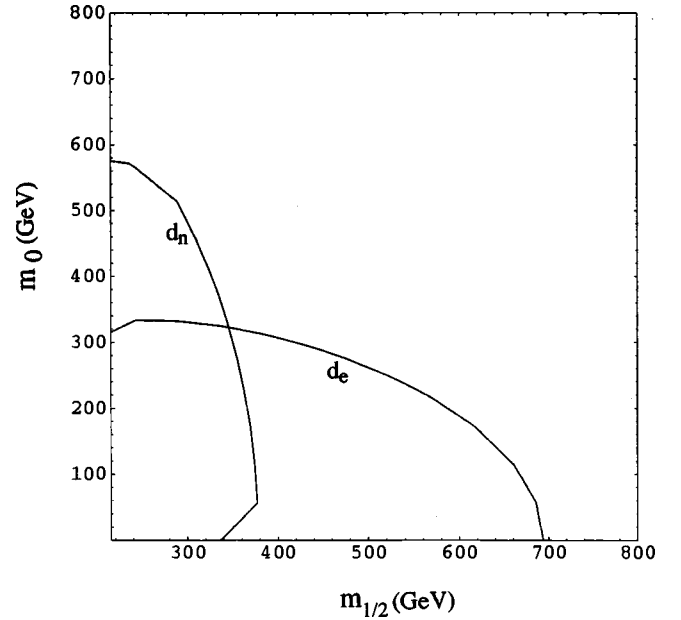

FIG. 15. Allowed region in the m_0-$m_{1/2}$ plane ($K \lesssim 0$) in a non-universal scenario. The other input parameters are $\alpha_{0A} = \pi/2$, $\theta_B = 0$, $|A_0| = 300$ GeV, $\tan\beta = 5$, $\delta_1 = 1$, $\delta_2 = -1$, $\delta_{10} = -1$, and $\delta_5 = -0.3$.

where $\theta = \epsilon_1 + \epsilon_2 + \theta_\mu$. Thus ϕ_1 effects any neutralino-chargino cancellations in d_e and d_n. An example is illustrated in Fig. 14. One sees that θ_B can be large, but is still tightly constrained to satisfy the experimental EDM bound (i.e., $\Delta \theta_B \simeq 0.02$). One is again led to a fine tuning at the GUT scale.

As an example of nonuniversal sfermion masses, we consider an SU(5)-type model where the GUT group possesses an SU(5) subgroup with matter embedded in the usual way in $10 + \bar{5}$ representations. We also assume that the first two generations remain universal to suppress flavor changing neutral currents. The Higgs boson masses have the form at M_G

$$m_{H_1}^2 = m_0^2 (1 + \delta_1), \quad m_{H_2}^2 = m_0^2 (1 + \delta_2), \tag{33}$$

while the third generation 10 representation (containing $\tilde{t}_L, \tilde{t}_R, \tilde{b}_L, \tilde{\tau}_R$) and the $\bar{5}$ (containing $\tilde{b}_R, \tilde{\nu}_\tau, \tilde{\tau}_L$) masses are parametrized by

$$m_{10}^2 = m_0^2 (1 + \delta_{10}), \quad m_{\bar{5}}^2 = m_0^2 (1 + \delta_s). \tag{34}$$

Here the $\delta_i \geq -1$ represent the deviations from the universality. In addition, the third generation cubic soft breaking parameters are A_{0t} and $A_{0b} = A_{0\tau}$.

One may use the non universal sfermion and Higgs boson masses to soften the effects of the experimental EDMs. This is illustrated in Fig. 15 where the $K = 0$ constraint is imposed in the m_0-$m_{1/2}$ plane for a choice of δ_i parameters. For $\delta_i = 0$, the d_n curve would continue to rise for small $m_{1/2}$ as seen in Fig. 9, rather than turn over as in Fig. 15. For example, for $m_{1/2} = 220$ GeV and $\tan\beta = 5$, $K(d_n) < 0$ occurs for $m_0 > 580$ GeV in the nonuniversal case, whereas $K(d_n)$

<0 occurs for $m_0 > 750$ GeV in the universal case. The particular set of $\delta_i s$ in the Fig. 15 is chosen to reduce the top and bottom squark mass and to satisfy the requirement of the radiative electroweak symmetry breaking. The lower top and bottom squark mass increases the Weinberg-type diagram which has a subtractive effect in the net EDM (NEDM) magnitude.

IV. SUGRA MODEL OF SMALL PHASES

While choosing the *CP* violating phases to be small, i.e., $\phi_i \simeq 10^{-2}$, to satisfy the EDM constraints appears to be artificial in the low energy MSSM, it is possible that a natural model of this type can arise in SUGRA GUT models.

SUGRA models depend on three functions of the chiral fields Φ_α: $f_{\alpha\beta}(\Phi_\alpha)$, the gauge kinetic energy: $K(\Phi_\alpha, \Phi_\alpha^\dagger)$, the Kähler potential; and $W(\Phi_\alpha)$, the superpotential. One assumes a hidden sector exists where some fields, e.g., moduli or dilaton, Φ_i grow VEVs of Planck size to break supersymmetry, i.e.,

$$x_i = \kappa \langle \Phi_i \rangle = O(1), \tag{35}$$

where $\kappa^{-1} = M_{Pl} = 2.4 \times 10^{18}$ GeV. Thus one can write $\{\Phi_\alpha\} = \{\Phi_i, \Phi_a\}$, where Φ_a are the physical sector fields. One might expand the Kähler potential in a power series of the physical fields:

$$K = \kappa^{-2} c^{(0)} + \left(c_{ab}^{(2)} \Phi_a \Phi_b + \frac{1}{M} c_{abc}^{(3)} \Phi_a \Phi_b \Phi_c + \cdots \right)$$
$$+ \left(\tilde{c}_{ab}^{(2)} \Phi_a \Phi_b^\dagger + \frac{1}{M} \tilde{c}_{abc}^{(3)} \Phi_a^\dagger \Phi_b \Phi_c + \cdots \right), \tag{36}$$

where M is a large mass. The $c^{(i)}, \tilde{c}^{(i)}$ are dimensionless, and we assume them to be $O(1)$. The first set of parentheses is holomorphic, and can be transferred to the superpotential by a Kähler transformation, giving rise to the μ term:

$$W \rightarrow W + \kappa^2 W \left(c_{ab}^{(2)} \Phi_a \Phi_b + \frac{1}{M} c_{abc}^{(3)} \Phi_a \Phi_b \Phi_c + \cdots \right). \tag{37}$$

The leading additional terms on the right occur when W there is replaced by its VEV $(\kappa^2 \langle W \rangle \simeq m_{3/2})$ and one of the fields in the cubic term, e.g., Φ_c, has a GUT scale VEV. Then $W \rightarrow W + \mu_{ab} \Phi_a \Phi_b$, where

$$\mu_{ab} = \left(c_{ab}^{(2)} + \frac{M_G}{M} c_{abc}^{(3)} \right) m_{3/2}. \tag{38}$$

In the perturbative heterotic string we expect $M \simeq M_{Pl}$ and hence $M_G/M \simeq O(10^{-2})$. If one assumes $c^{(2)}$ is real and $c^{(3)}$ is complex with arbitrary size phase, then μ naturally has a phase of size $\theta_{0\mu} \simeq O(10^{-2})$. A similar analysis can be done for the other parameters $(A, B, \tilde{m})$ yielding automatically small phases. One assumes only that the leading (renormalizable) term in the matter expansion is real, while the higher terms (presumably arising from integrating out the tower of massive states) can have arbitrary phases.

Other string scenarios can have $M \simeq O(M_G)$. In that case one expects the nonrenormalizable terms to give rise to large phases, unless the low lying members of the tower of heavy states do not couple to the fields of the physical sector.

V. CONCLUSIONS

In SUGRA GUT models, the basic parameters are given at the GUT scale. The renormalization group equations then carry this information to the electroweak scale, allowing for experimental tests of the model. Thus what represents a "natural" choice of parameters is presumably a GUT scale question.

The experimental values of the electric dipole moments put strong constraints on the low energy SUSY parameter space. However, for MSUGRA models at least, the RGEs suppress the value of the A_t phase at the electroweak scale, α_t, so that any size of phase, α_{0A}, even $\pi/2$ at M_G will generally lead to acceptable EDMs. This effect is due to the nearness of the t quark to its Landau pole.

The EDMs, however, are very sensitive to the B phase at the electroweak scale, θ_B. In the domain of the light SUSY mass spectrum (i.e., $\lesssim 1$ TeV) and $\alpha_{0A} \simeq O(1)$, the EDMs allow a large θ_B [i.e., $O(10^{-1})$] only for low $\tan\beta$, i.e., $\tan\beta \lesssim 3$. Further, for fixed SUSY parameters in this domain, the allowed range $\Delta\theta_B$ of θ_B needed to satisfy the EDM constraints is very small for $\tan\beta \gtrsim 3$.

The above results strongly affect the GUT theory. Thus for α_{0A} large and a light mass spectrum, one finds at the GUT scale that θ_{0B} is generally large, i.e., $O(1)$ even for low $\tan\beta$, and the allowed range $\Delta\theta_{0B}$ for satisfying the EDMs is exceedingly small for $\tan\beta \gtrsim 3$. Thus, for this situation, θ_{0B} must be chosen large and be very precisely determined as $\tan\beta$ gets large, leading to a new fine tuning problem at the GUT scale. The origin of this difficulty resides in the requirement that the GUT models give rise to parameters at the electroweak scale that simultaneously satisfy the experimental EDM constraints and give rise to radiative electroweak breaking.

The above discussion suggests that reasonable MSUGRA models with large phases and mass spectrum below 1 TeV can only be constructed for small $\tan\beta$, i.e., $\tan\beta \lesssim 3$. The current LEP data combined with cosmological constraints already require $\tan\beta \gtrsim 2$ [43], and LEF, the Tevatron, and the LHC will be able to explore the domain $\tan\beta \lesssim 50$ [44]. Thus the value of $\tan\beta$ (or a lower bound) is something that will be determined experimentally in the not too distant future. Should $\tan\beta$ turn out to be large, it is possible that only models with small GUT phases $\phi_{0i} \simeq O(10^{-2})$ are reasonable, and it was shown above that such models can arise naturally with $\phi_{0i} \simeq O(M_G/M_{Pl})$.

Our analysis has included the loop corrections to the radiative breaking condition. While these corrections are small, they grow with $\tan\beta$ and are competitive to the θ_B contribution to the EDMs. Thus, for large $\tan\beta$ (e.g., $\tan\beta \simeq 20$), they can produce a new cancellation phenomena (with $\theta_B = 0$), allowing the EDM constraints to be satisfied for a light mass spectra (e.g., $m_0 \simeq 300$ GeV, $m_{1/2} \simeq 200$ GeV), which for lower $\tan\beta$ would be excluded by the EDM data.

The combined restrictions of the experimental EDM bounds for the neutron and electron put strong constraints on the SUSY parameter space. However, since the theoretical cancellations needed to satisfy experiment are delicate, as one varies the parameters one can get rather different excluded regions. Thus, while we have found that increasing m_0 gives an allowed region of smaller $m_{1/2}$ (as one might have expected), increasing $|A_0|$ can require $m_{1/2}$ to be increased to satisfy the EDM bounds. However, it should be stressed that there are significant theoretical uncertainties in the calculation of d_n, and we have seen, for example, that the current uncertainty in the quark masses m_u and m_d (arising from the uncertainty in m_s) can lead to a significant variation in the domain the neutron EDM data can exclude. Alternate methods of calculating d_n [28,29] would be expected to shift the location in parameter space satisfied by the simultaneous constraints from the electron and neutron EDMs. However, the basic conclusion that the θ_{0B} is fine tuned at the GUT scale would not be changed, since this is required from considering only the electron EDM (the difficulty being exacerbated if both the electron and the neutron EDM constraints are imposed).

Much of the above discussion holds also for non minimal models with nonuniversal gaugino and sfermion soft breaking masses. A more detailed discussion of the effects of non-universalities will be given elsewhere [41].

ACKNOWLEDGMENTS

[1] J. Ellis, S. Ferrara, and D. V. Nanopoulos, Phys. Lett. **114B**, 231 (1982); W. Buchmuller and D. Wyler, *ibid.* **121B**, 321 (1983); J. Polchinski and M. B. Wise, *ibid.* **125B**, 393 (1983).

[2] E. Commins *et al.*, Phys. Rev. A **50**, 2960 (1994); K. Abdullah *et al.*, Phys. Rev. Lett. **65**, 2347 (1990).

[3] P. G. Harris *et al.*, Phys. Rev. Lett. **82**, 904 (1999).

[4] J.-M. Gerard *et al.*, Nucl. Phys. **B253**, 93 (1985); E. Franco and M. Mangano, Phys. Lett. **135B**, 445 (1984); A. Sanda, Phys. Rev. D **32**, 2992 (1985); M. Dugan, B. Grinstein, and L. Hall, Nucl. Phys. **B255**, 413 (1985); W. Bernreuther and M. Suzuki, Rev. Mod. Phys. **63**, 313 (1991).

[5] P. Nath, Phys. Rev. Lett. **66**, 2565 (1991); Y. Kizukuri and N. Oshimo, Phys. Rev. D **45**, 1806 (1992); **46**, 3025 (1992); R. Garisto and J. Wells, *ibid.* **55**, 1611 (1997).

[6] T. Ibrahim and P. Nath, Phys. Lett. B **418**, 98 (1998).

[7] T. Ibrahim and P. Nath, Phys. Rev. D **57**, 478 (1998).

[8] T. Ibrahim and P. Nath, Phys. Rev. D **58**, 111301 (1998).

[9] T. Falk and K. Olive, Phys. Lett. B **439**, 71 (1998).

[10] S. Barr and S. Khalil, Phys. Rev. D **61**, 035005 (2000).

[11] T. Falk, K. Olive, M. Pospelov, and R. Roiban, Nucl. Phys. **B560**, 3 (1999).

[12] M. Brhlik, G. Good, and G. Kane, Phys. Rev. D **59**, 115004 (1999).

[13] M. Brhlik, L. Everett, G. Kane, and J. Lykken, Phys. Rev. Lett. **83**, 2124 (1999).

[14] A. Bartl, T. Gajdosik, W. Porod, P. Stockinger, and H. Stremnitzer, Phys. Rev. D **60**, 073003 (1999).

[15] S. Pokorski, J. Rosiek, and C. A. Savoy, Nucl. Phys. **B570**, 81 (2000).

[16] D. Demir, Phys. Rev. D **60**, 055006 (1999).

[17] A. Pilaftsis and C. Wagner, Nucl. Phys. **B553**, 3 (1999).

[18] T. Falk, A. Ferstl, and K. Olive, Phys. Rev. D **59**, 055009 (1999).

[19] T. Falk, K. Olive, and M. Srednicki, Phys. Lett. B **375**, 196 (1996).

[20] U. Chattopadhyay, T. Ibrahim, and P. Nath, Phys. Rev. D **60**, 063505 (1999).

[21] A. Pilaftsis, Phys. Rev. D **58**, 096010 (1998); Phys. Lett. B **435**, 88 (1998).

[22] A. Chamseddine, R. Arnowitt, and P. Nath, Phys. Rev. Lett. **49**, 970 (1982); for reviews, see P. Nath, R. Arnowitt, and A. Chamseddine, *Applied N=1 Supergravity* (World Scientific, Singapore, 1984); H. P. Nilles, Phys. Rep. **110**, 1 (1984).

[23] E. Cremmer, S. Ferrara, L. Girardello, and A. Van Proeyen, Phys. Lett. **116B**, 231 (1982); Nucl. Phys. **B212**, 413 (1983).

[24] E. Witten and J. Bagger, Nucl. Phys. **B222**, 125 (1983).

[25] D. Chang, W-Y. Keung, and A. Pilaftsis, Phys. Rev. Lett. **82**, 900 (1999).

[26] Dai *et al.*, Phys. Lett. B **237**, 216 (1990).

[27] R. Arnowitt, J. L. Lopez, and D. V. Nanopoulos, Phys. Rev. D **42**, 2423 (1990); R. Arnowitt, M. Duff, and K. Stelle, *ibid.* **43**, 3085 (1991).

[28] M. Ramsey-Musolf, Phys. Rev. Lett. **83**, 3997 (1999).

[29] J. Donoghue, E. Golowich, and B. Holstein, Phys. Rep. **131**, 319 (1986).

[30] A. Manohar and H. Georgi, Nucl. Phys. **B234**, 189 (1984).

[31] H. Leutwyler, Phys. Lett. B **374**, 163 (1996).

[32] R. Gupta and T. Bhattacharya, Phys. Rev. D **55**, 7203 (1997); B. Gough *et al.*, Phys. Rev. Lett. **79**, 1622 (1997).

[33] R. Burkhalter, Nucl. Phys. B (Proc. Suppl.) **73**, 3 (1999).

[34] L. E. Ibanez and C. Lopez, Nucl. Phys. **B233**, 511 (1984); L. E. Ibanez, C. Lopez, and C. Munoz, *ibid.* **B256**, 218 (1985).

[35] CLEO Collaboration, M. S. Alam *et al.*, Phys. Rev. Lett. **74**, 2885 (1995).

[36] S. Bertolini, F. Borzumati, A. Masiero, and G. Ridolfi, Nucl. Phys. **B353**, 591 (1991); J. Wu, R. Arnowitt, and P. Nath, Phys. Rev. D **51**, 1371 (1995); V. Barger, M. Berger, P. Ohmann, and R. Phillips, *ibid.* **51**, 2438 (1995).

[37] A. Dedes, A. Lahanas, and K. Tamvakis, Phys. Rev. D **59**, 015019 (1999).

[38] V. Barger, M. Berger, and P. Ohmann, Phys. Rev. D **49**, 4908 (1994).

[39] P. Nath, J. Wu, and R. Arnowitt, Phys. Rev. D **52**, 4169 (1995).

[40] G. Gamberini, G. Ridolfi, and F. Zwirner, Nucl. Phys. **B331**, 331 (1990); R. Arnowitt and Pran Nath, Phys. Rev. D **46**, 3981 (1992).

[41] E. Accomando, R. Arnowitt, and B. Dutta, Phys. Rev. D **61**, 075010 (2000).

[42] S. Abel and J. Frere, Phys. Rev. D **55**, 1623 (1997); A. Masiero and H. Murayama, Phys. Rev. Lett. **83**, 907 (1999); K. S. Babu, B. Dutta, and R. N. Mohapatra, Phys. Rev. D **61**, 091701 (2000); S. Khalil and T. Kobayashi, Phys. Lett. B **460**, 341 (1999).

[43] J. Ellis, T. Falk, K. Olive, and M. Srednicki, hep-ph/9905481.

[44] M. Carena, S. Mrenna, and C. Wagner, hep-ph/9907422.